Medical Engineering and Physics 000 (2016) 1–14

Contents lists available at ScienceDirect

Medical Engineering and Physics

journal homepage: www.elsevier.com/locate/medengphy

Upper-limb stroke rehabilitation using electrode-array based functional electrical stimulation with sensing and control innovations

M. Kutlu[a,*], C.T. Freeman[a], E. Hallewell[b,c], A-M. Hughes[b], D.S. Laila[d]

[a] Electronics and Computer Science, Faculty of Physical Sciences and Engineering, University of Southampton, UK
[b] Faculty of Health Sciences, University of Southampton, UK
[c] Faculty of Health and Social Science, Bournemouth University, UK
[d] Faculty of Engineering and the Environment, University of Southampton, UK

ARTICLE INFO

Article history:
Received 10 December 2014
Revised 11 January 2016
Accepted 31 January 2016
Available online xxx

Keywords:
Stroke rehabilitation
Functional electrical stimulation
Iterative learning control
Sensing technology

ABSTRACT

Functional electrical stimulation (FES) has shown effectiveness in restoring upper-limb movement post-stroke when applied to assist participants' voluntary intention during repeated, motivating tasks. Recent clinical trials have used advanced controllers that precisely adjust FES to assist functional reach and grasp tasks with FES applied to three muscle groups, showing significant reduction in impairment. The system reported in this paper advances the state-of-the-art by: (1) integrating an FES electrode array on the forearm to assist complex hand and wrist gestures; (2) utilising non-contact depth cameras to accurately record the arm, hand and wrist position in 3D; and (3) employing an interactive touch table to present motivating virtual reality (VR) tasks. The system also uses iterative learning control (ILC), a model-based control strategy which adjusts the applied FES based on the tracking error recorded on previous task attempts. Feasibility of the system has been evaluated in experimental trials with 2 unimpaired participants and clinical trials with 4 hemiparetic, chronic stroke participants. The stroke participants attended 17, 1 hour training sessions in which they performed functional tasks, such as button pressing using the touch table and closing a drawer. Stroke participant results show that the joint angle error norm reduced by an average of 50.3% over 6 attempts at each task when assisted by FES.

1. Introduction

Stroke is the principal cause of adult disability in the UK, with an annual incidence of 152,000 people [1]. Approximately 70% of survivors experience altered arm function after a stroke, and 40% are left with a non-functional arm [2]. The upper extremity (UE) is fundamental to activities of daily living (ADLs) [3] with the ability to reach and grasp required in over 50% of activities [4]. The capacity to achieve ADLs has a direct impact on independence, reducing the social and financial burden of stroke. Complete recovery of UE function is predicted in only 11.6% of patients [5] and unequivocal evidence shows that intense training can significantly improve outcomes post-stroke [6]. Consequently there is a move towards technology that facilitates activity in the upper limb and provides specific and intense rehabilitation which could, potentially, be implemented independently of a therapist.

Technology-assisted training of arm-hand skills with functional electrical stimulation (FES) is an attractive treatment option because it can potentially deliver intensive periods of treatment with comparatively little demand on resources [2]. A wide body of evidence supports FES in improving range of movement (both passively and actively), strength and spasticity [7–9]. It is also well established that FES has a positive effect on motor control [8,10]. Neuroplastic changes are greater if the practice method is meaningful, repetitive and intensive in nature [6,7,11]. Assistive technologies, including FES, together with task-orientated training combines two rehabilitation paradigms for the UE, providing a means to enable patients to practise meaningful, functional tasks more intensely and more effectively on their own. Statistical evidence shows that benefits of FES are greatest when combined with maximum voluntary effort from the patient [8,12,13]. It is hence important for an FES system to accurately assist functional tasks while encouraging user effort.

Model based feedback control is critical to reduce the effects of noise/disturbance by adjusting the FES according to achieved motion, measuring using sensor data. This facilitates significant increase in accuracy and enables complex tasks to be performed.

* Corresponding author. Tel.: +44 2380596651.
E-mail addresses: mck1e12@ecs.soton.ac.uk, mck1e12@soton.ac.uk (M. Kutlu), cf@ecs.soton.ac.uk (C.T. Freeman), eh6e11@soton.ac.uk (E. Hallewell), A.Hughes@soton.ac.uk (A-M. Hughes), D.Laila@soton.ac.uk (D.S. Laila).

http://dx.doi.org/10.1016/j.medengphy.2016.01.004
1350-4533/

Although, many model-based FES control strategies have been employed to control movement [14], most are designed for Spinal Cord Injury (SCI) subjects, and have a strong focus on the lower limb. The complexity of the musculo-skeletal system and the difficulty of muscle selectivity and recruitment means that fewer approaches have been applied to the UE [15]. The great majority of the UE systems that have been clinically trialled employ feed-forward or triggered control [16,17]. Electromyography (EMG) has also been successfully employed [18], but it is delayed and is not always suitable for neurological conditions due to discoordination or weakness. However, a small number of clinically trialled UE rehabilitation systems employ feedback control [19] including an adaptive controller for the hand and wrist [20], and proportional-integral-derivative controllers for the shoulder and elbow joints which are applied in conjunction with a support that sequentially restricts motion to a single joint in turn [21]. Greater accuracy has been shown through incorporation of model information within the controller. For example, Artificial Neural Network (ANN) approaches have been used to approximate nonlinear components of the dynamic system within feedback control schemes [22], giving rise to asymptotic tracking capability. However, ANNs require retraining for different tasks and often lack robust stability guarantees.

One of the few model-based control approaches to be employed in clinical trials is iterative learning control (ILC). ILC operates by comparing movement data from a previous attempt at a task to an idealised reference trajectory for the same task. After each attempt it uses the model to adjust the level of stimulation given to each muscle group with a view to reducing the tracking error on the subsequent attempt. This iterative process applies the minimum level of FES for task attainment while simultaneously encouraging voluntary contribution from the participant. Previous studies combining FES and ILC have demonstrated feasibility of using single pad electrodes to deliver precisely controlled stimulation to the anterior deltoid, triceps and wrist extensors [23–25].

Recently, use of transcutaneous electrode arrays has been shown to address limitations of single pad electrode such as selectivity, automated placement, fatigue and discomfort [26,27]. These also have been found to enable participants to perform a variety of functional tasks including walking [28,29], and hand and wrist motion [30]. However, existing control strategies use time-consuming element selection procedures followed by open-loop control, limiting the resulting accuracy.

The system developed in this paper combines electrode-arrays with model-based ILC in order to train goal-oriented tasks. This is the first system to use model-based FES control of an array within an upper-limb stroke rehabilitation system. The system embeds innovations in the stimulation hardware, sensing equipment, control algorithms, and task display, including:

1. A 24 element electrode array (Fatronik-Tecnalia Inc., Spain) placed over the wrist and finger extensors that enables functional hand gestures to be performed.
2. A PrimeSense Carmine 1.09 (Apple Inc., California) depth camera that uses an RGB camera and infrared sensor to measure hand and wrist joint angles, reducing set-up time and removing constraints associated with contact-based sensors (e.g. goniometers).
3. A capacitive touch table (DISPLAX Inc., Portugal) that displays each task in an interactive manner.

These new developments promote further reduction in upper limb motor impairments, as reflected by evidence that functional improvement from training is mostly restricted to the actually trained functions and activities [31]. In addition, the touch table promotes adherence through stimulating and motivating rehabilitation, as required in long term self-management. Its combination with inexpensive non-contact depth sensors represents a significant step towards translation into the home environment.

2. System overview

The system comprises five components (see Fig. 1). Participants sit on a perching stool in front of a touch table, and a SaeboMAS arm support (Saebo Inc., Charlotte) is used to de-weight their upper extremity according to individual need. Surface electrodes are positioned on the anterior deltoid and triceps, and an electrode array is placed over the common extensor complex of the forearm. The PrimeSense is used in combination with another depth camera (Kinect; Microsoft Washington) to measure the position of joint centres within the shoulder, elbow and wrist. Data from these sensors are fed into the control algorithm hardware and software, which updates the FES control signals for each muscle group to

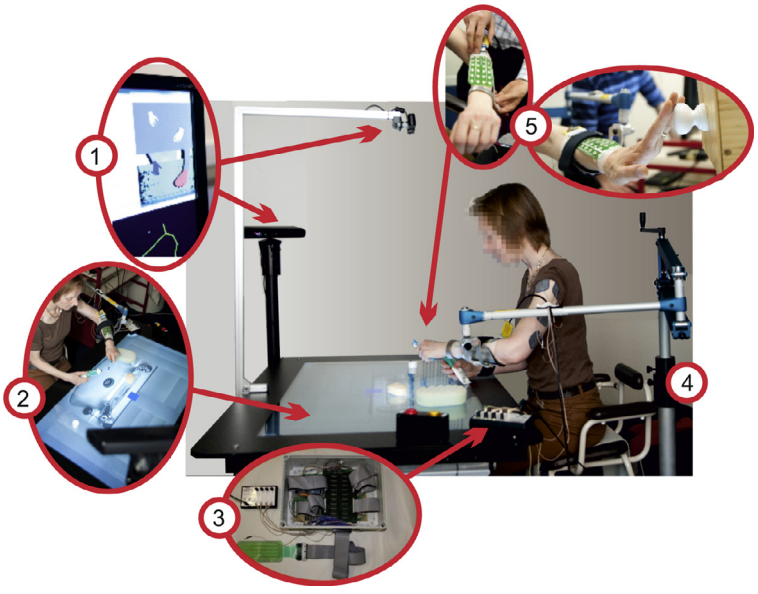

Fig. 1. System components: (1) Motion tracking hardware components, (2) interactive touch table display, (3) FES controller and multiplexor hardware, (4) SaeboMAS and perching stool, and (5) electrode-array.

Please cite this article as: M. Kutlu et al., Upper-limb stroke rehabilitation using electrode-array based functional electrical stimulation with sensing and control innovations, Medical Engineering and Physics (2016), http://dx.doi.org/10.1016/j.medengphy.2016.01.004

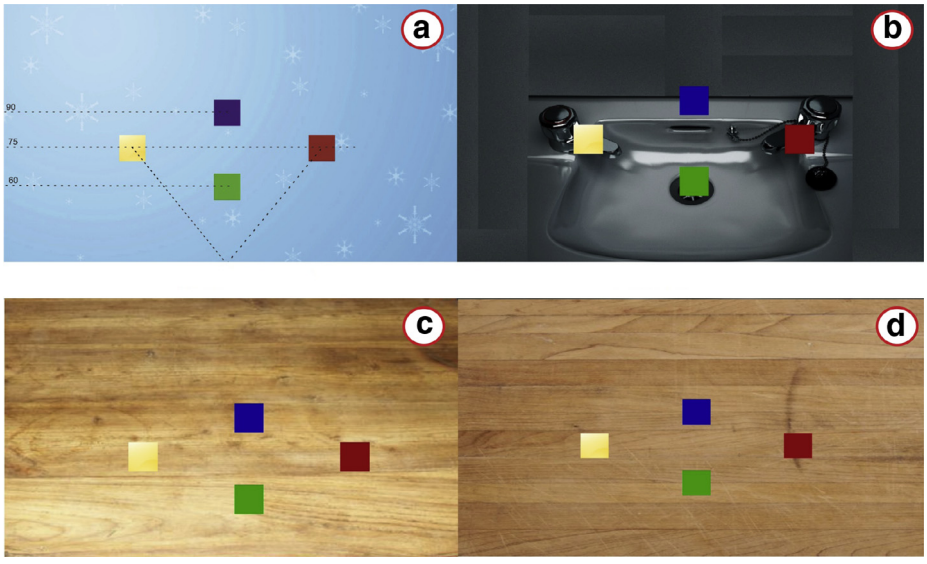

Fig. 2. Task design and graphical backgrounds: (a) default (overlaid with task placement geometry), (b) bathroom sink, (c) coffee table and (d) chopping board.

provide just enough electrical stimulation to assist performance of functional tasks. These tasks include picking up a tube of toothpaste, and moving the item to a different position on a representation of a sink displayed by the touch table. The therapist uses an operator monitor displaying a graphical user interface (GUI) to select appropriate tasks and monitor training progression. The therapist also has an over-ride stop button which can be used to terminate trials with immediate effect.

2.1. Task design

Functional tasks that are typically performed in everyday life were designed to offer a range of reaching challenges across the workspace. Fig. 2 shows the four main images used on the touch table background; a default image, a bathroom sink, a coffee table, and a chopping board. Tasks comprised reaching, grasping and manipulating real objects relevant to each image. There are five main tasks; closing a drawer, switching on a light switch, stabilising an object, button pressing and repositioning an object. The light switch is located at two different heights (low and high) and there are four table-mounted positions at which the virtual buttons can be located or real objects repositioned both in the sagittal plane and towards the frontal plane (45° across body, 45° to the hemiplegic side or in line with the shoulder) as illustrated in Fig. 2. The objects are placed at different percentages of arm length (60%, 75%, and 90%) from the participant's glenohumeral joint as shown in Fig. 2a). The table was positioned at a distance of 45% arm length from the glenohumeral joint and 35 cm below the arm when the arm was held 90° horizontal to the shoulder.

2.2. System software

The software and data flow is shown schematically in Fig. 3. The system software undertakes tracking of the participant's movement in real-time, extraction of kinematic variables, and subsequent implementation of control schemes to adjust the FES in real-time. A custom made C++ application interfaces with Kinect middle-ware (Skeletal Viewer), which in turns receives data from PrimeSense via a Client/Server (Transmission Control Protocol (TCP)) connection with its associated middle-ware (3Gear Systems). This application

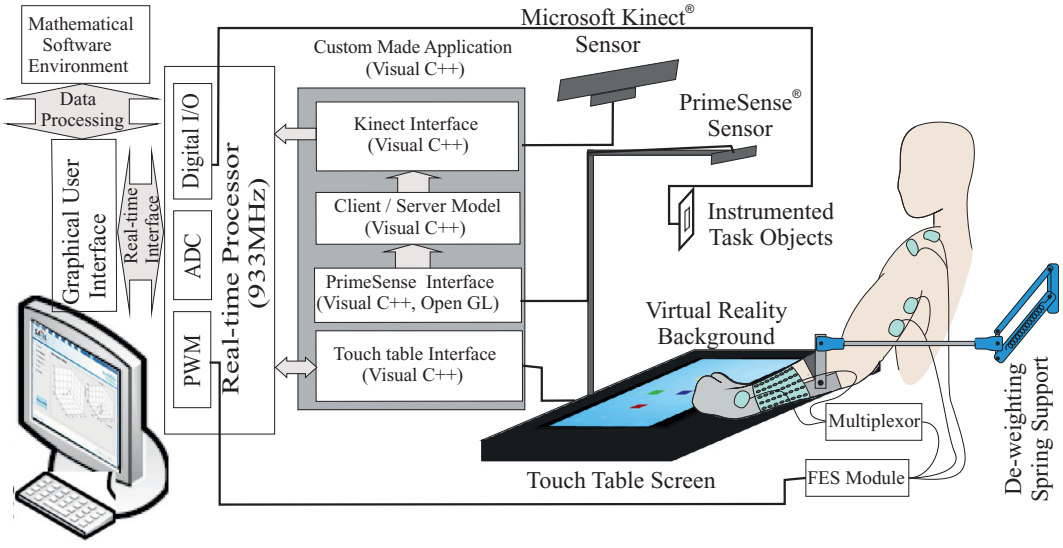

Fig. 3. Software signal flow diagram.

Please cite this article as: M. Kutlu et al., Upper-limb stroke rehabilitation using electrode-array based functional electrical stimulation with sensing and control innovations, Medical Engineering and Physics (2016), http://dx.doi.org/10.1016/j.medengphy.2016.01.004

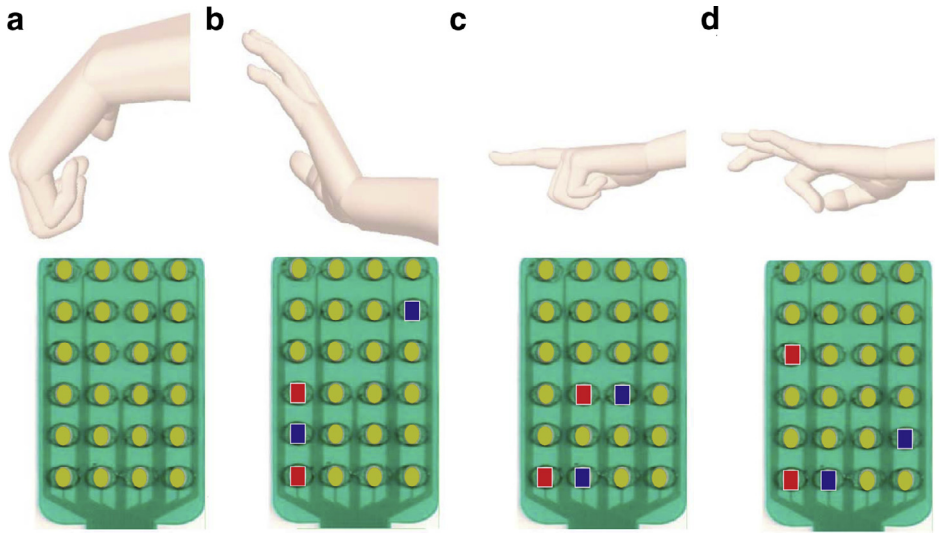

Fig. 4. Experimental hand gestures and identified array elements (left hand view): (a) Starting, (b) Open hand, (c) Pointing, and (d) Pinch gestures.

directly communicates with real-time hardware (dSPACE ds1103), which handles all data processing and control implementation, and interfaces with the touch table and graphical user interface (GUI) via direct hardware access. Communication with the touch table employs Snowflake software (NUITEQ Inc., Sweden) which controls the task display and touch feedback. The GUI oversees communication with the system inputs and outputs and is responsible for customising control parameters, implementing the FES control, collecting and storing position data, selecting the task to be performed and reviewing performance after each session. The real-time hardware generates pulse-width modulated (PWM) signals for each of the FES stimulator channels, together with RS232 serial data to control the electrode array. Digital inputs and outputs are also employed to interface with the instrumented task objects.

2.3. FES hardware

The FES hardware comprises single pad electrodes, an electrode array, and electronic components to generate and route stimulation signals. The single pad FES surface electrodes are positioned on the anterior deltoid and triceps muscles, with placement following clinical guidelines [32]. Similarly the electrode array is placed on the forearm to actuate wrist and hand extensor muscles. The electrode array is manufactured by Tecnalia-Fatronik, San Sebastian, Spain, and is described in [29]. It comprises 4 × 6 elements printed on a polycarbonate substrate, using a continuous interface layer consisting of a 0.89 mm thick layer of Axelgaard AG603 hydrogel. A separate 5 cm × 5 cm anodal electrode is located above the styloid process of the ulna. Each array element can be routed to two of the four available FES channels via custom-made RS232 controlled multiplexor hardware, comprising an Arduino board and shift register array which interface with a relay bank. The optimal electrode sites are selected for each required hand and wrist posture relevant to tasks of daily living, using an optimisation procedure described in Section 2.7. These postures are shown in Fig. 4 and comprise open-hand and pinching movements for grasping and releasing objects, and a pointing movement for switching lights and pushing buttons. The array stimulation sites are then fixed during subsequent experiments, with the four stimulation channels controlled using real-time algorithms, as described in Section 2.6. For each FES channel, the control hardware produces a 5 V, 40 Hz pulse train, where pulse-width is the controlled variable (0–300 μ s). These are then fed to a four channel stimulator (Odstock Medical Ltd., Salisbury, UK) which amplifies the voltage of each channel to a fixed level which is determined at the beginning of each session. The voltage amplitude is set by applying a 300 μ s signal to the stimulation site and slowly increasing a dial on the stimulator until the maximum comfortable level is achieved. When setting the voltage amplitude of an array channel, the stimulation site comprises two adjacent array elements located over the wrist and hand extensor muscles.

2.4. Motion tracking

To accurately assist functional UE movement requires precise feedback control of appropriate joint angles. There are a variety of low-cost position sensing approaches that are suitable for home-use and can be used by patients with minimal assistance. Kinect is a popular sensor platform for rehabilitation [33,34] and provides shoulder, elbow and wrist joint positions with an accuracy of approximately 10 mm [35,36]. However, it provides only a single joint position for the hand and bespoke software developed to extract finger joint location measurements severely restricts the range of admissible movement [37]. Therefore, the system also incorporates PrimeSense to collect the wrist position data and individual finger joint centre position data via commercial 3Gear middle-ware. Although there is evidence that using two Kinects can cause interference, this has been found to have little effect on measurement and is strongly correlated with the distance between sensors and observed object [38]. To examine sensor efficacy, joint error has been recorded during repeated tests performed using the proposed training task set, and performance has been quantified through comparison with a goniometer. A maximum joint error of less than 10° has been established with the Kinect placed at 45° on the opposite side of the impaired arm at a −20° pitch angle in sitting mode, and the PrimeSense positioned 700 mm above the touch-table.

The model employed in this research is a substantial development of UE models used in previous FES-based stroke rehabilitation research [24], and includes a comprehensive hand description. Joint centres and corresponding joint angles are shown in Figs. 4 and 5, respectively. The Kinect is used to capture joint centre locations $(x_i,\ y_i,\ z_i)^\top$ for the shoulder, elbow and wrist, $i = 1, 2, 3$, respectively. The PrimeSense captures joint centre locations $(x_i,\ y_i,\ z_i)^\top$ for the hand and wrist, $i = 3 \ldots 18$, respectively. Joint angles $\phi_1,\ \cdots \phi_5$ denote the orientation of the upper arm and forearm segments, with joint axes that are chosen to align with the motion elicited by FES. The procedure

Please cite this article as: M. Kutlu et al., Upper-limb stroke rehabilitation using electrode-array based functional electrical stimulation with sensing and control innovations, Medical Engineering and Physics (2016), http://dx.doi.org/10.1016/j.medengphy.2016.01.004

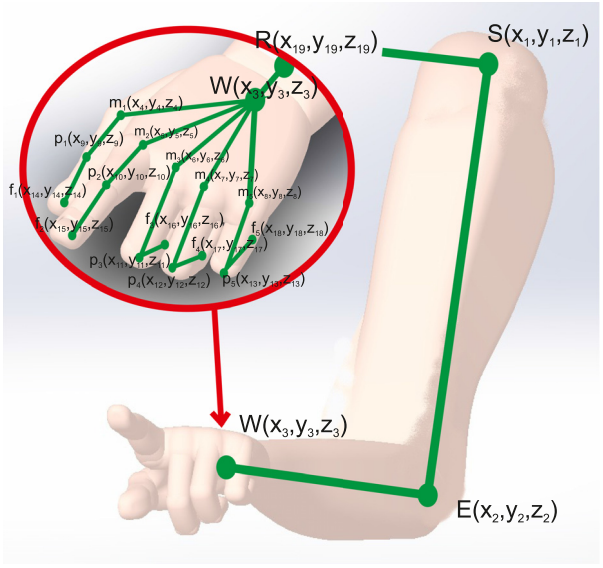

Fig. 5. Human arm joint centre locations.

employed to define $\phi_1, \ldots \phi_5$ is described in [39], together with the mapping $\left((x_1, y_1, z_1)^\top, \ldots, (x_3, y_3, z_3)^\top\right) \mapsto (\phi_1, \ldots, \phi_5)$. The position vectors $(x_i, y_i, z_i)^\top$ are denoted by W and R for the wrist $(i = 3)$ and root $(i = 18)$ respectively with m, p and f similarly denoting the metacarpophalangeal (MCP) joint positions, proximal interphalangeal (PIP) joint positions and fingertip positions, respectively. Note that the model does not include the distal interphalangeal joints due to their limited range of movement. Using these data, the wrist flexion/extension and abduction/adduction joint angles are then computed respectively by

$$\phi_6 = \arccos\left(\frac{\vec{RW}\cdot\vec{Wm}_3}{|\vec{RW}||\vec{Wm}_3|}\right),$$
$$\phi_7 = \arccos\left(\frac{\vec{RW}\times\vec{Wm}_3}{|\vec{RW}||\vec{Wm}_3|}\cdot\frac{\vec{m_5m_3}}{|\vec{m_5m_3}|}\right) - 90^\circ. \quad (1)$$

The MCP joints angles, ϕ_8 to ϕ_{12}, and PIP joints, ϕ_{13} to ϕ_{17}, are similarly computed respectively by

$$\phi_{13-i} = \arccos\frac{\vec{Wm_i}\cdot\vec{m_ip_i}}{|\vec{Wm_i}||\vec{m_ip_i}|},$$
$$\phi_{18-i} = \arccos\frac{\vec{p_if_i}\cdot\vec{p_if_i}}{|\vec{p_if_i}||\vec{p_if_i}|}, \quad i = 1, \ldots, 5. \quad (2)$$

2.5. Biomechanical model

The controller updates the stimulation signal applied to each muscle group with the aim of reducing the error in performing each task from one attempt to the next. The control signal is generated using kinematic joint information, in combination with a biomechanical dynamic model of the stimulated arm, given by

$$B_h(\Phi)\ddot{\Phi} + C_h(\Phi, \dot{\Phi})\dot{\Phi} + F_h(\Phi, \dot{\Phi}) + G_h(\Phi) = \tilde{g}(u, \Phi, \dot{\Phi}) - J^\top(\Phi)h \quad (3)$$

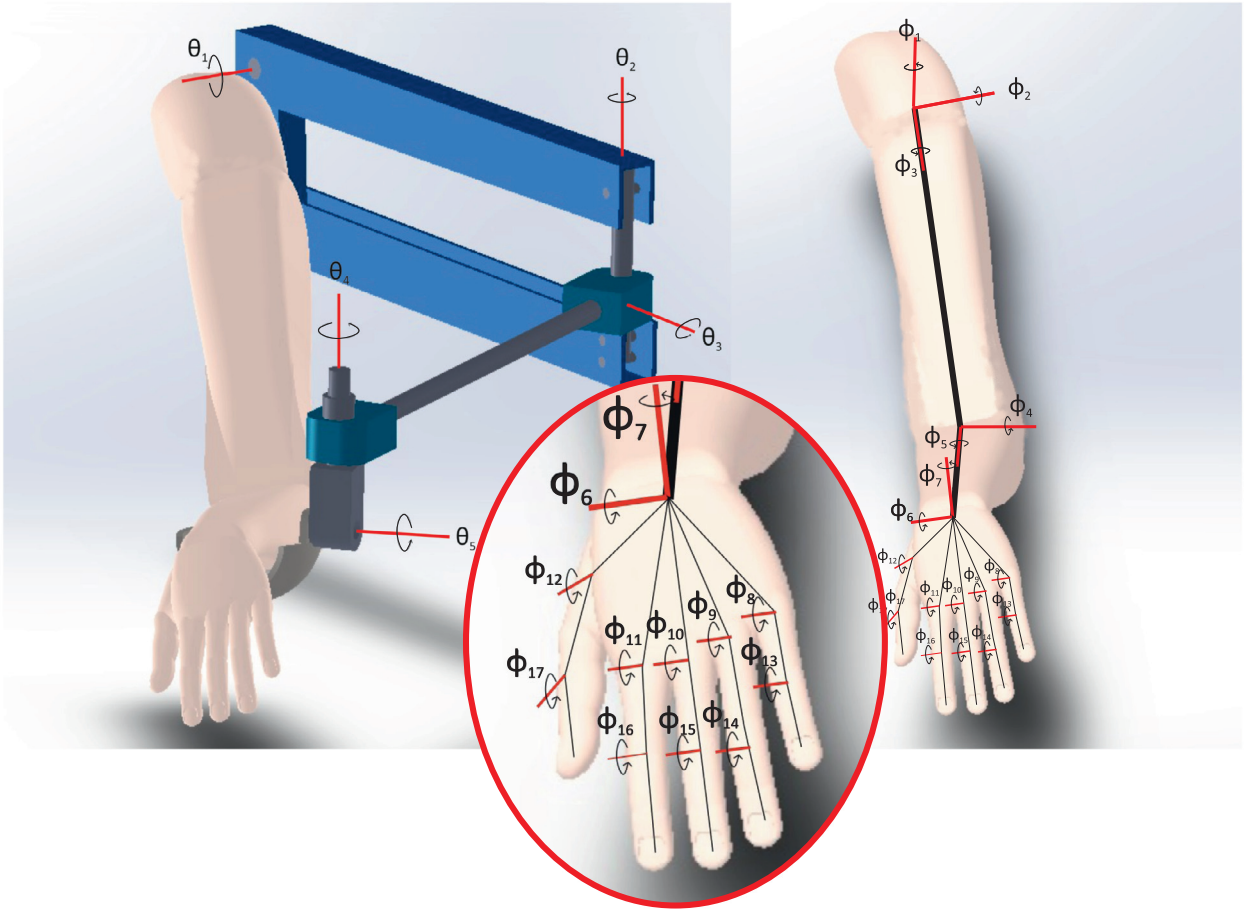

Fig. 6. Human arm kinematic model.

where $B_h(\cdot)$ and $C_h(\cdot)$ are 17-by-17 inertial and Coriolis matrices, respectively, $F_h(\cdot)$ and $G_h(\cdot)$ are friction and gravitational vectors, h is a vector of external force and torque due to interaction with objects, and $J(\Phi)$ is the system Jacobian. The vectors $\Phi = [\phi_1, \ldots, \phi_{17}]^\top$ and $u = [u_1, u_2, u_3, u_4]^\top$ respectively denote joint angles and applied electrical stimulation, where $u_1(t)$ and $u_2(t)$ represent the electrical stimulation pulse-width signals applied to the anterior deltoid and triceps muscles respectively, and $u_3(t)$ and $u_4(t)$ represent the electrical stimulation pulse-width signals that are routed to elements within the electrode array at time t. The vector $\tilde{g}(\cdot)$, comprising the resulting moments produced through application of FES, has form

$$\tilde{g}(u, \Phi, \dot{\Phi}) = [\tilde{g}_1(u, \Phi, \dot{\Phi}), \ldots, \tilde{g}_{17}(u, \Phi, \dot{\Phi})]^\top. \quad (4)$$

The moments produced through stimulation of the anterior deltoid and triceps take the form $\tilde{g}_2(u, \Phi, \dot{\Phi}) = g_2(u_1, \phi_2, \dot{\phi}_2)$ and $\tilde{g}_4(u, \Phi, \dot{\Phi}) = g_4(u_2, \phi_4, \dot{\phi}_4)$, respectively. The components associated with the unassisted upper arm and forearm joint angles are given by $\tilde{g}_i(u, \Phi, \dot{\Phi}) = 0$, $i = 1, 3, 5$.

The stimulation signal that is transmitted to the 24 elements of the array is given by $\mu(t) = [\mu_1(t), \ldots, \mu_{24}(t)]^\top = W[u_3(t), u_4(t)]^\top$ where matrix $W \in \mathbb{R}^{24\times 2}$ has elements which are determined as 0 or 1 by the relay hardware. When stimulated, it is assumed that each element of the electrode array may produce a moment about any of the hand and wrist joint axes, leading to the form

$$\tilde{g}_i(u, \Phi, \dot{\Phi}) = \sum_{j=1}^{24} \tilde{g}_{i,j}(\mu_j(t), \phi_i, \dot{\phi}_i), \quad i = 6, \ldots, 17. \quad (5)$$

Moments generated about ϕ_4, ϕ_5 can similarly be added to $\tilde{g}_i(\cdot)$, $i = 4, 5$ but have been found to be negligible. For the same reason, the effect of ϕ_4, ϕ_5 on $\tilde{g}_i(\cdot)$, $i = 6, \ldots, 17$ has been neglected. From [40], the moments in (4) generated by stimulation of the anterior deltoid and triceps take the general forms

$$\begin{aligned} g_2(u_1(t), \phi_2, \dot{\phi}_2) &= h_2(u_1, t) \times F_{m,2}(\phi_2, \dot{\phi}_2), \\ g_4(u_2(t), \phi_4, \dot{\phi}_4) &= h_4(u_2, t) \times F_{m,4}(\phi_4, \dot{\phi}_4). \end{aligned} \quad (6)$$

where $h_i(u_i, t)$ is a Hammerstein structure incorporating a static non-linearity, $h_{IRC,i}(u_i)$, that represents the isometric recruitment curve, cascaded with linear activation dynamics, $h_{LAD,i}(t)$. The term $F_{m,i}(\phi, \dot{\phi})$ models the multiplicative effect of the joint angle and joint angular velocity on the active torque developed by the muscle. Due to weakness, spasticity and fatigue, stroke patients commonly experience slow restricted movement in their hand and wrist. This means the multiplicative effect of angle and angular velocity can be neglected since it is approximately unity [41]. The moment around axis i due to stimulation of electrode array element j is accordingly given by

$$\tilde{g}_{i,j}(\mu_j(t), \phi_i, \dot{\phi}_i) = h_{i,j}(\mu_j, t), \quad i = 6, \ldots, 17, \quad j = 1, \ldots, 24. \quad (7)$$

where $h_{i,j}(\mu_j, t)$ is a Hammerstein structure incorporating a static non-linearity, $h_{IRC,i,j}(\mu_j)$, that represents the isometric recruitment curve, cascaded with linear activation dynamics, $h_{LAD,i}(t)$. Inserting (7) into (5) yields

$$\tilde{g}_i(u, \Phi, \dot{\Phi}) = g_i(\mu(t), \phi_i, \dot{\phi}_i) = h_i(\mu, t), \quad i = 6, \ldots, 17 \quad (8)$$

where $h_i(\mu, t)$ is a composite Hammerstein structure incorporating nonlinearity $h_{IRC,i}(\mu) = \sum_{j=1}^{24} h_{i,j}(\mu_j, t)$, cascaded with linear activation dynamics, $h_{LAD,i}(t)$. The SaeboMAS support structure has the form

$$B_s(\Theta)\ddot{\Theta} + C_s(\Theta, \dot{\Theta})\dot{\Theta} + F_s(\Theta, \dot{\Theta}) + G_s(\Theta) + K_s(\Theta) = 0 \quad (9)$$

where vector $\Theta = [\theta_1, \ldots, \theta_5]^\top$ contains the joint angles of the spring support, $B_s(\cdot)$ and $C_s(\cdot)$ are 5-by-5 inertial and Coriolis matrices, and $F_s(\cdot)$ and $G_s(\cdot)$ are friction and gravitational vectors respectively. Vector $K_s(\cdot)$ comprises the moments produced through gravity compensation provided by the spring, which takes form $[k_1(\theta_1), 0, 0, 0, 0]^\top$. When connected to arm structure (3), a bijective mapping between joint angles, $\Theta = M(\Phi)$, yields the combined model

$$\begin{aligned} &B(\Phi)\ddot{\Phi} + C(\Phi, \dot{\Phi})\dot{\Phi} + F(\Phi, \dot{\Phi}) + G(\Phi) + K(\Phi) \\ &\quad = \tilde{g}(u, \Phi, \dot{\Phi}) - J^\top(\Phi)h \end{aligned} \quad (10)$$

where

$$\begin{aligned} B(\Phi) &= B_h(\Phi) + M_1(\Phi)^\top B_s(M(\Phi))M_1(\Phi), \\ G(\Phi) &= G_h(\Phi) + M_1(\Phi)^\top G_s(M(\Phi)), \\ C(\Phi, \dot{\Phi}) &= C_h(\Phi, \dot{\Phi}) + M_1(\Phi)^\top C_s(M(\Phi), M_1(\Phi)\dot{\Phi})M_1(\Phi), \\ K(\Phi) &= M_1(\Phi)^\top K_s(M(\Phi)), \\ F(\Phi, \dot{\Phi}) &= F_h(\Phi, \dot{\Phi}) + M_1(\Phi)^\top F_s(M(\Phi), M_1(\Phi)\dot{\Phi}) \\ &\quad + M_1(\Phi)^\top B_s(M(\Phi))M_2(\Phi, \dot{\Phi})\dot{\Phi} \end{aligned}$$

with $M_1(\Phi) = \frac{dM(\Phi)}{d\Phi}$ and $M_2(\Phi, \dot{\Phi}) = \frac{d}{dt}(\frac{dM(\Phi)}{d\Phi})$. This model is next used by the FES control system.

2.6. Control scheme

The combined human arm and support dynamics (10) are shown in Fig. 7, where the moments due to muscle activation are $g_a(u_a, \Phi_a, \dot{\Phi}_a) := [0, g_2(u_1, \phi_2, \dot{\phi}_2), 0, g_4(u_2, \phi_4, \dot{\phi}_4), 0]^\top$ and $g_w(\mu, \Phi_w, \dot{\Phi}_w) := [g_6(\mu, \phi_6, \dot{\phi}_6), \ldots, g_{17}(\mu, \phi_{17}, \dot{\phi}_{17})]^\top$. Here $u_a = [u_1, u_2]^\top$ is the stimulation applied to the shoulder and elbow, and $u_w = [u_3, u_4]^\top$ is the stimulation applied to the forearm muscles via the multiplexor and electrode array, so that $\mu = Wu_w$. In addition, $\Phi_a = [\phi_1, \ldots, \phi_5]^\top$ and $\Phi_w = [\phi_6, \ldots, \phi_{17}]^\top$ contain the joint angles of the upper arm and wrist, respectively. The reach and grasp tasks consist of repeated movements for the participant's affected arm, with a rest period in between, during which their arm is returned to a common starting position. The reference $\hat{\Phi}(t) = [\hat{\phi}_1(t), \ldots, \hat{\phi}_{17}(t)]^\top$ contains the desired joint angles over the trial duration $t \in [0, T]$. The feedback controller is partitioned as $C_c = \mathrm{diag}\{C_{c,a}, C_{c,w}\}$ and designed to establish stability and baseline tracking over each trial. The requirement to repeatedly perform a set of finite duration tasks with a fixed initial arm position enables ILC to be utilised to improve tracking performance. ILC uses the performance error from each trial to update the input $v_k = [v_{a,k}^\top, v_{w,k}^\top]^\top$ in an attempt to increase the accuracy of the subsequent attempt. On trial k, $\Phi_k(t)$ denotes the joint angles and the associated error is given by $e_k = \hat{\Phi} - \Phi_k$.

Identification methods have been developed in previous research to establish parameters within a model of the form (10) containing joints $\phi_1, \ldots, \phi_5$, with the hand and wrist treated as a lumped mass (see Section 2.7). This model information means that controller $C_{c,a}$ can be selected to take the form $C_{c,a} = M_a K_a(s)$ where M_a: $x \mapsto u_a$ is an input–output linearising controller which introduces an auxiliary control input x and enforces dynamics $\phi_i(s) = H_a(s)x_i(s)$, $i = 2, 4$, where $H_a(s) = \frac{1}{s^5}$. Feedback controller $K_a(s) = [0, K_{a,2}(s), 0, K_{a,4}(s), 0]^\top$ is then selected to stabilise the resultant closed-loop dynamics

$$\begin{aligned} &G_{a,i} : (\hat{\phi}_i + v_{k,i}) \mapsto \phi_{k,i} : \phi_{k,i}(s) \\ &\quad = (I + H_a(s)K_{a,i}(s))^{-1}H_a(s)K_{a,i}(s)(\hat{\phi}_i(s) + v_{k,i}(s)), \quad i = 2, 4. \end{aligned} \quad (11)$$

Implementation of M_a requires joint angles, angular velocities and estimated muscle states, with full details given in [42], which contains experimental results confirming satisfactory closed-loop performance in the presence of modelling uncertainty. It is also supported by detailed robustness analysis [43]. The uncontrolled joint

Please cite this article as: M. Kutlu et al., Upper-limb stroke rehabilitation using electrode-array based functional electrical stimulation with sensing and control innovations, Medical Engineering and Physics (2016), http://dx.doi.org/10.1016/j.medengphy.2016.01.004

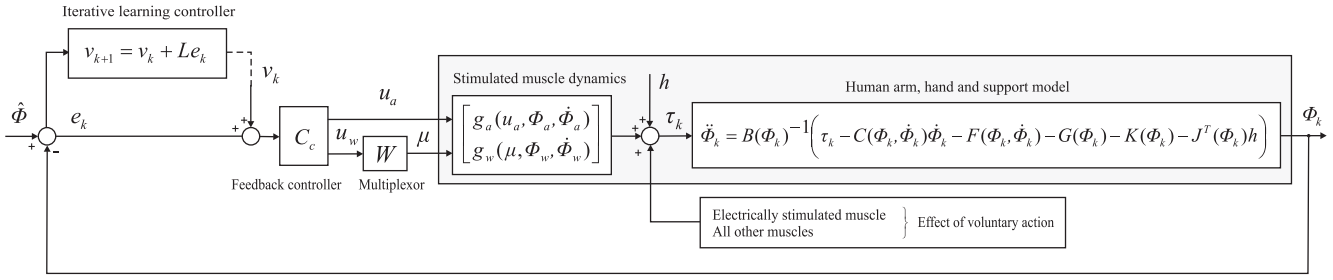

Fig. 7. Block diagram of the ILC feedback scheme with $L = \text{diag}\{L_a, L_w\}$ and $C_c = \text{diag}\{C_{c,a}, C_{c,w}\}$. Note, the dashed line denotes computer memory updating of ILC signal v_k.

angles ϕ_1, ϕ_3 and ϕ_5 are assumed to be under the patient's remaining voluntary control, however analysis in [42] confirms that interaction with controlled variables does not destabilise the system given sufficient damping and stiffness.

Due to the close proximity of muscles in the hand and wrist, and the difficulty in measuring forces, it is not feasible to extend the global upper arm model identification approaches to include the hand and wrist. Therefore a linearised model $H_w(s) : \mu_k \mapsto \Phi_{w,k}$ is identified about a suitable operating point, as described in Section 2.7. Feedback controller $C_{c,w} = K_w(s)$ is then chosen to stabilise system $H_w(s)W$ to yield the resulting closed-loop dynamics

$$G_w : (\hat{\Phi}_w + v_{w,k}) \mapsto \Phi_w : \Phi_w(s) = (I + H_w(s)WK_w(s))^{-1}H_w(s)WK_w(s)(\hat{\Phi}_w(s) + v_{w,k}(s)). \quad (12)$$

Many possible designs for $H_w(s)$ exist, with the form presented in Appendix A providing guaranteed error tracking properties and stability across all joints, Φ_w.

Having stabilised the arm dynamics, an ILC scheme is implemented in order to provide input v_k such that the error is minimised, i.e. $\lim_{k\to\infty} v_k = v_k^\star$ with $v_k^\star := \min_{v_k} \|\hat{\Phi} - \Phi_k\|^2$. This is achieved through the update structure

$$v_{k+1} = v_k + Le_k, \qquad v_0 = 0, \quad k = 0, 1, \ldots \quad (13)$$

where $L = \text{diag}\{L_a, L_w\}$. Inserting (11) and (12) into (13), together with $e_k(t) = [e_{a,k}(t)^\top,\ e_{w,k}(t)^\top]^\top$ and $\hat{\Phi}(t) = [\hat{\Phi}_a(t)^\top,\ \hat{\Phi}_w(t)^\top]^\top$ yields relationships

$$\begin{aligned} e_{a,k+1} &= (I - G_aL_a)e_{a,k}, \\ e_{w,k+1} &= (I - G_wL_w)e_{w,k}, \\ v_{a,k+1} &= (I - L_aG_a)v_{a,k} + L_a(I - G_a)\hat{\Phi}_a, \\ v_{w,k+1} &= (I - L_wG_w)v_{w,k} + L_w(I - G_w)\hat{\Phi}_w. \end{aligned} \quad (14)$$

For the arm dynamics, design of $L_{a,i}$ to satisfy $\|I - G_{a,i}L_{a,i}\| < 1$, $i = 2, 4$, guarantees convergence of ϕ_i to zero error, and many suitable schemes are available, see [30] and examples therein. The equivalent relationship, $\|I - G_wL_w\| < 1$, guarantees convergence of Φ_w to zero error, but cannot be satisfied due to the restricted range of operator G_w. Instead L_w can be designed to satisfy $\|I - L_wG_w\| < 1$ which guarantees convergence of error $e_{w,k}$ to the limiting solution $\left(I - G_w(L_wG_w)^{-1}L_w\right)\hat{\Phi}_w$. Appropriate selection of L_w can hence minimise the error norm, and is detailed in Appendix A. In both cases a robust ILC scheme can deal with dynamic changes and modelling inaccuracy due to fatigue, spasticity and other time-varying physiological effects, with robust uncertainty bounds given in [44].

2.7. Model identification

Identification of the upper arm component of (10) firstly involves identifying the stimulated joint axes within the kinematic model (Fig. 6) described in Section 2.4. This is achieved by applying a ramped 10 s FES signal to the anterior deltoid and fitting a plane to the resulting movement. Transformations are then embedded in the kinematic chain to align ϕ_2 with the identified axis, with all the other axes defined as in Section 2.4. Identification of the arm and shoulder dynamics follows the procedure described in [42] in which external forces are applied to the arm using a torque/force sensor and an optimisation procedure performed.

Numerous methods can be used to identify the hand and wrist dynamics $H_w(s) : \mu_k \mapsto \Phi_{w,k}$ around an operating point which corresponds to the kth trial, including fitting a linear model to the trial data set $\{\mu_k,\ \Phi_k\}$ (see [44] for analysis of resulting stability), or selecting a model from a set identified over a range of operating points at the beginning of the treatment session. In Appendix A feedback and ILC structures have been proposed for the case where the hand and wrist dynamics assume the structure of $H_w(s) = \bar{H}_w(s)P$ comprising uniform dynamics and a 24 × 12 static mapping. In this case P can be identified by applying a slow triangular ramp profile to each array element in turn and fitting a line to the resulting joint movement. Dynamics $H_w(s)$ are then identified by stimulating all elements with a single input sequence, μ, and fitting a single linear model to the combined data $\{\Phi_w, P\mu\}$. Matrix W is then computed by solving $\min_{W,u} \|\hat{\Phi}_w - \bar{H}_wPWu\|^2$ for reference trajectories corresponding to open hand, pointing and pinching. The matrix W then defines the electrode array element-stimulator mapping for each gesture type, with representative identified elements shown in Fig. 4. Further details of the identification process appear in [30].

Table 1
Stroke participant demographic characteristics.

Participant	Gender	Age (years)	Side of paresis	Time since stroke
1	M	54	L	35 months
2	M	51	L	64 months
3	F	47	L	60 months
4	M	43	L	96 months
Average		48.75		63.75 months

3. Experimental evaluation

The system has been tested with both unimpaired and stroke participants. Following ethical approval, 6 participants (2 unimpaired and 4 stroke) were recruited with demographic characteristics for the latter given in Table 1. At the beginning of each session they were set-up at the workstation, which took approximately 15 min and comprised: 1) participant placement as described in Section 2, 2) electrode-array and single electrode placement and setting of comfortable stimulation amplitude for each channel as described in Section 2.3, 3) dynamic model identification as described in Section 2.7.

Please cite this article as: M. Kutlu et al., Upper-limb stroke rehabilitation using electrode-array based functional electrical stimulation with sensing and control innovations, Medical Engineering and Physics (2016), http://dx.doi.org/10.1016/j.medengphy.2016.01.004

Each unimpaired participant attended a single session, in which they used the system to perform the tasks described in Section 2.1. They were instructed to provide no voluntary effort, and were not shown the task. Each stroke participant attended 17 intervention sessions. The inclusion criteria were: (i) aged 18 years old or over; (ii) stroke causing hemiplegia of at least 6 months duration; (iii) impaired upper limb that includes the inability to effectively extend the elbow in reaching and impaired opening and closing of the hand; (iv) FES produces movement through a functional range; (v) able to comply with study protocol that includes ability to position arm at start point of each trial; (vi) able to communicate effectively; (vii) able to provide written informed consent. The exclusion criteria for participants were: (i) any active device implant; (ii) a metal implant in the affected upper limb; (iii) uncontrolled epilepsy; (iv) pregnancy and lactation; (v) any serious or unstable medical, physical or psychological condition or cognitive impairment that would compromise the subject's safety or successful participation in the study; (vi) requirement of an interpreter; (vii) current participation in another study involving physical rehabilitation of the arm. The set-up procedure also followed steps (1) to (3) above, and was followed by 60 min practising of a subset of FES-assisted functional reach and grasp tasks dictated by clinical need. At the beginning and end of each intervention session, each stroke participant completed two tasks without FES assistance (high light switch and button pressing tasks). Clinical assessments, described in Section 3.2.3, were carried out before and after the intervention. The assessments were conducted according to standard protocol, by qualified physiotherapists who were independent of the study. Data collection was carried out by a team of experienced researchers.

3.1. Unimpaired participant results

The model identification procedure of Section 2.7 was followed using the simplified $H_w(s)$ structure. In principle the hand and wrist identification procedure must be repeated for a range of operating points. However, due to the dominant effect of spasticity and stiffness outweighing variation in operating point conditions, satisfactory results were obtained by performing a single identification test at the start of each session. $K_a(s)$ was selected as a proportional controller, yielding $C_{c,a} = M_a K_a(s)$, where input-linearising controller M_a was implemented using the identified arm dynamics. The feedback controller $C_{c,w} = K_w(s) = \bar{K}_w(s)(PW)^\dagger$ of Appendix A was employed, with $\bar{K}_w(s)$ selected as a proportional plus derivative controller. The resulting closed-loop dynamics $G_a(s)$ and $G_w(s)$ are given by (11) and (12) respectively, where the latter simplifies to the form (A.3). These were then used to design ILC operators L_a and L_w respectively within ILC update (13). For simplicity phase-lead structures were selected due to their ease of tuning and previous successful use in clinical trials [24]. This produces $L_a(s) = l_a \text{diag}\{0,1,0,1,0\} e^{s\lambda_a}$, and from (A.7) the form $L_w(s) = l_w (PW)^\dagger e^{s\lambda_w}$. These correspond to the update

$$\underbrace{\begin{bmatrix} v_{a,k+1}(t) \\ v_{w,k+1}(t) \end{bmatrix}}_{v_{k+1}(t)} = \underbrace{\begin{bmatrix} v_{a,k}(t) \\ v_{w,k}(t) \end{bmatrix}}_{v_k(t)} + \begin{bmatrix} l_a \begin{bmatrix} 0 & & & & \\ & 1 & & & \\ & & 0 & & \\ & & & 1 & \\ & & & & 0 \end{bmatrix} & \\ & l_w (PW)^\dagger \end{bmatrix} \times \begin{bmatrix} e_{a,k}(t+\lambda_a) \\ e_{w,k}(t+\lambda_w) \end{bmatrix}, \quad \lambda_a, \lambda_w > 0. \tag{15}$$

Tests comprised 6 trials of each of the far reaching and low light switch tasks. SaeboMAS support was set individually for each participant at the minimum level, which enable them to satisfactorily complete the task when also assisted by FES. This meant they could contribute maximum voluntary effort, whilst not being demotivated. In practice, this level was achieved heuristically by the therapist based on a clinical experience and was adjusted based on task difficulty, fatigue and spasticity. Results for Participant 1, as illustrated by Fig. 8, confirm improved tracking between trials $k = 1$ and $k = 6$ with summary performance measures given in Table 2. Here ϕ_2 and ϕ_4 are the controlled shoulder and elbow axes, and, although all wrist and hand axes were controlled, emphasis has been placed on ϕ_6 and ϕ_{11} (wrist and index finger extension) angles as 42% of the functional movements of the hand involve the four fingers moving together [4]. Reference trajectory $\hat{\Phi}$ was extracted in separate tests with 12 unimpaired participants, as reported in [45,46].

For the anterior deltoid and triceps proportional gains were chosen between 2 and 3. For the forearm muscles proportional gains were chosen between 1 and 1.2 and derivative gains were between 0.3 and 0.5. These were selected so that closed loop dynamics $G_a(s)$ and $G_w(s)$ approximate a pure delay, and hence emphasis was placed on reducing oscillation and following the shape of a delayed copy of the reference. The pure delays could then be removed by the ILC algorithm by setting them equal to the phase-leads, yielding $l_a = 0.3$ and $\lambda_a = 0.8\,s$, $l_w = 0.3$ and $\lambda_w = 0.8\,s$. The effect of fatigue and moderate to severe spasticity was addressed by re-tuning the feedback control parameters, and reducing learning gains λ_a, λ_w to sacrifice convergence speed for robustness. Results confirm satisfactory tracking accuracy of the FES-controlled joint angles ϕ_2, ϕ_4, ϕ_6 and ϕ_{11}, and hence feasibility of the system in supports those joints most relevant to stroke participants. Note that, since these unimpaired participants supplied no voluntary input this assistance did not necessary translate into accurate completion of overall task (which would be expected in the case of stroke participants since they typically maintain control over the unassisted joint angles).

3.2. Stroke participant results

For each stroke participant the set-up procedure steps (1) to (3) were performed at the beginning of each of the 17 intervention sessions, using the same identification procedure and control structures as the unimpaired case. Identification of the anterior deltoid axis, and the hand and wrist dynamics, was performed each session, since these components are highly dependent on electrode placement and hence vary widely between sessions. However, the arm and shoulder dynamics took far longer to identify but varied less widely (note that their dependence on support level can easily be accounted for by prior characterisation of $K_s(\theta)$ for different support settings without recourse to re-identification). Therefore, due to time constrains their identification was not repeated each session unless performance was deemed unsatisfactory, which occurred only once. The four chronic participants each completed the intervention over 6–8 weeks.

3.2.1. FES-unassisted results

During FES-unassisted tasks each participant was only supported by gravitational support. The level of support was set by the physiotherapist at a constant level during the first treatment session according to each participant's needs. The range of movement, defined as the difference between maximum and minimum joint angles, was calculated for each FES-unassisted task. Results in Table 4 demonstrate improved range of movement at all four stimulated joints over the intervention. In particular mean improvements over the course of the intervention were 5° in shoulder

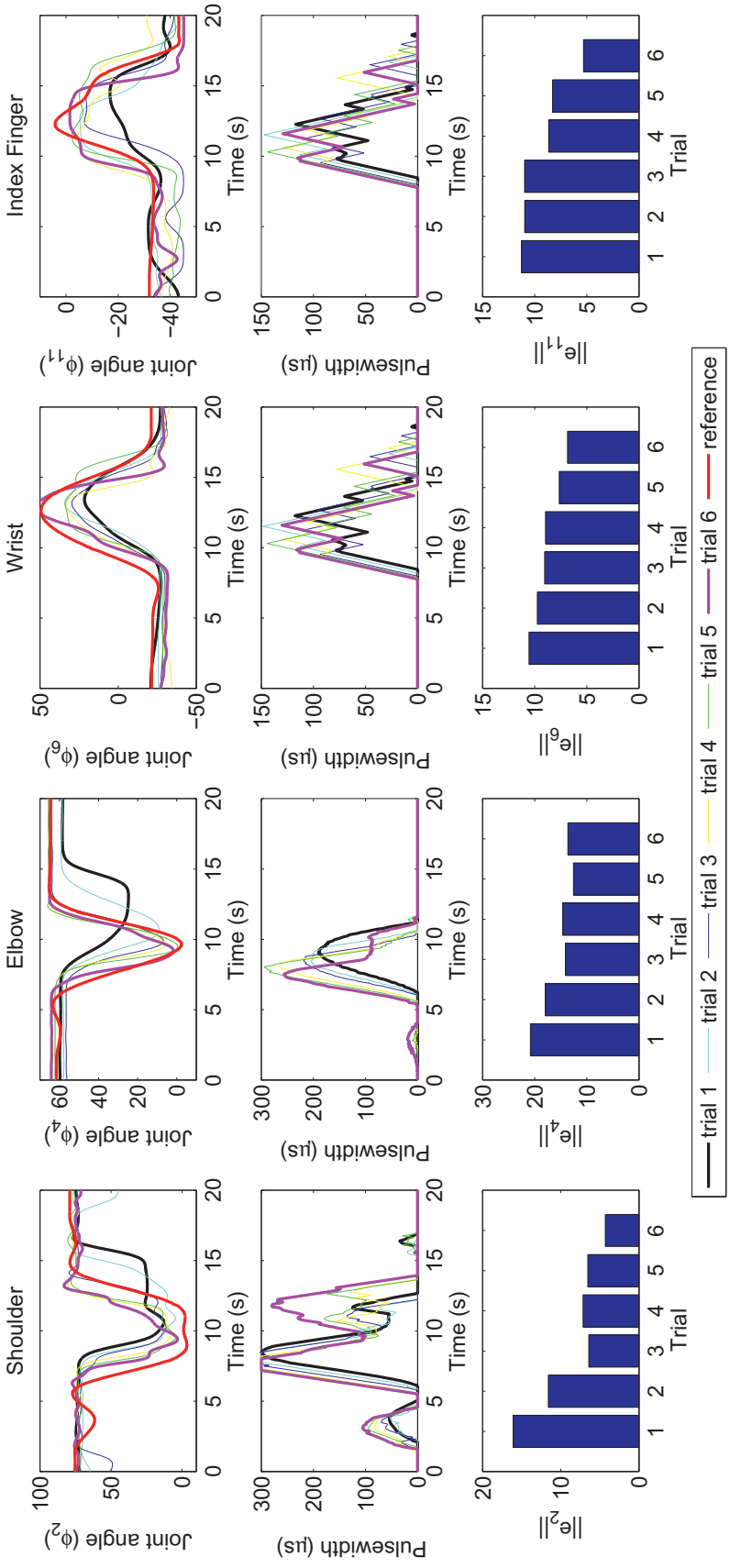

Fig. 8. Unimpaired Participant 1's tracking results for far reach task.

Table 2
Unimpaired participants assisted results.

	Task	Trial no	Norm of error			
			$\|\hat{\phi}_2 - \phi_2\|$	$\|\hat{\phi}_4 - \phi_4\|$	$\|\hat{\phi}_6 - \phi_6\|$	$\|\hat{\phi}_{11} - \phi_{11}\|$
Participant 1	Far reaching	1	8.54	8.72	12.76	8.51
		6	3.45	6.34	6.55	5.02
	Low light switch	1	9.95	11.33	6.12	3.73
		6	4.33	3.68	4.95	3.02
Participant 2	Far reaching	1	12.09	6.86	8.49	7.05
		6	7.92	4.68	4.90	4.99
	Low light switch	1	7.30	7.03	19.58	12.38
		6	2.03	6.42	6.60	8.17

flexion (high light switch), 13° in elbow extension (contralateral reach), 42° in wrist extension (near reach), and 34° in index finger extension (far reach). Two-tailed paired t-tests were applied to the base-line and post intervention mean range of movement values and yielded p-values < 0.05 for three of the four cases.

3.2.2. FES-assisted results

When assisted by FES, each participant was supported by both gravitational support and FES according to their clinical need. The level of gravitational support was varied between tasks based on physiotherapist observations and participant voluntary action. For all participants the level reduced over the intervention. As shown in Figs. 9 and 10 improvements were seen in mean tracking accuracy for all four joints as was the case with unimpaired participants. The results demonstrate the success of the control system for improving movement accuracy during reaching and grasping tasks. Summary performance measures are given in Table 3 and confirm that tracking accuracy increased between the first and last ILC trials. For example, the norm of tracking error for all joints (last column) decreased by 50.3%, attaining an accuracy on trial $k = 6$ which confirms that the overall movement was performed to a satisfactory level of precision to support functional movement. Since the first trial ($k = 1$) corresponds to $v_k = 0$, these results clearly show the improvement compared with using proportional and proportional plus derivative feedback controllers alone.

3.2.3. Clinical assessments

The primary outcome measures were the motor component of the Fugl-Meyer assessment (FM) and the Action Research Arm Test (ARAT), with maximum scores of 66 and 57, respectively. Scores are shown in Table 4 with improvements seen in both; for two participants the ARAT and for three participants the FM improved.

4. Discussion

This research is motivated by findings showing that shoulder and elbow training only improves motor impairment in the shoulder and elbow [23,25], similarly training of the wrist and finger extensors only improves hand function [47]. However, when these muscle groups are trained simultaneously, significant improvements are observed, with participants reporting greater capacity to perform everyday tasks at home, such as opening drawer, stabilising and moving objects, and pressing light switches [24]. Unfortunately current home-based systems stimulate too few muscles and use non-selective, large electrodes. They also do not employ position feedback or model based control algorithms. This leads to inadequate support during functional activities.

The aim of this study is to establish the feasibility of combining state-of-the-art technologies to enable people with stroke to practise goal-oriented functional tasks. The system developed in this paper incorporates VR, FES hardware, advanced sensing, control and passive support. Compared with previous systems, this demonstrates a substantial development in the scope of technology for upper-limb rehabilitation.

A critical element of the system reported in this paper is an electrode array and advanced model-based control scheme that supports activities of daily living. Use of such arrays is an emerging area, however published control approaches typically involve sequentially activating subsets of elements, evaluating the resulting movement, and finally selecting those elements that most closely approximate the desired movement [26,28,48]. This process is time-consuming and leads to inaccurate motion due to open loop control action in which stimulation is not subsequently updated in response to physiological changes. In contrast, ILC has been shown capable of providing precise control of hand and wrist movement by employing a dynamic model of the hand and wrist, and learning from past experience [30,39,42]. The tuning process can also be implemented in less than 30 s [30]. In this study the model-based array ILC framework is integrated into the system to produce fine finger movements during training of everyday tasks. While the study confirmed acceptance and positive outcomes, limitations included the small sample size, absence of a control group or follow-up (due to time constraints).

A number of further developments are required before the system can be transferred to patients' own homes:

1. Expensive components (dSpace and touch table) can readily be replaced with affordable alternatives (an embedded hardware (e.g. NI myRIO-1950) and a tablet).
2. The sensor accuracy limitation highlighted in Section 2.4 can be addressed by employing recent hardware updates (such as Kinect v2 which can replace both depth cameras and thereby reduce infrared interference).
3. The control scheme can be made autonomous to reduce set-up time, enable use without an engineer, and adapt to physiological changes such as fatigue and spasticity. A major challenge is to eliminate the need to perform model identification tests, which are not feasible for the home environment, especially without the assistance of a carer. A possible solution is to employ the multiple model adaptive framework established in [49] which incorporates a large number of 'candidate' model representations which feasibly represent the system dynamics. It evaluates the fitting accuracy using a Kalman filter bank, and switches the controller corresponding to the most accurate model into closed loop. Robust performance banks are reported in [44], and initial results when applied to FES control of the UE are given in [49]. Using this approximation, the models identified in this paper therefore can be used to populate the candidate model set.
4. If necessary, the SaeboMAS can be replaced with a more affordable alternative (e.g. Bakx Magic Arm, Focal Meditech Balancer, Sammons Preston Stable Slide). Their dynamics can also be represented in the form (9), and the new combined structure (10) is used to construct the candidate model set.

Please cite this article as: M. Kutlu et al., Upper-limb stroke rehabilitation using electrode-array based functional electrical stimulation with sensing and control innovations, Medical Engineering and Physics (2016), http://dx.doi.org/10.1016/j.medengphy.2016.01.004

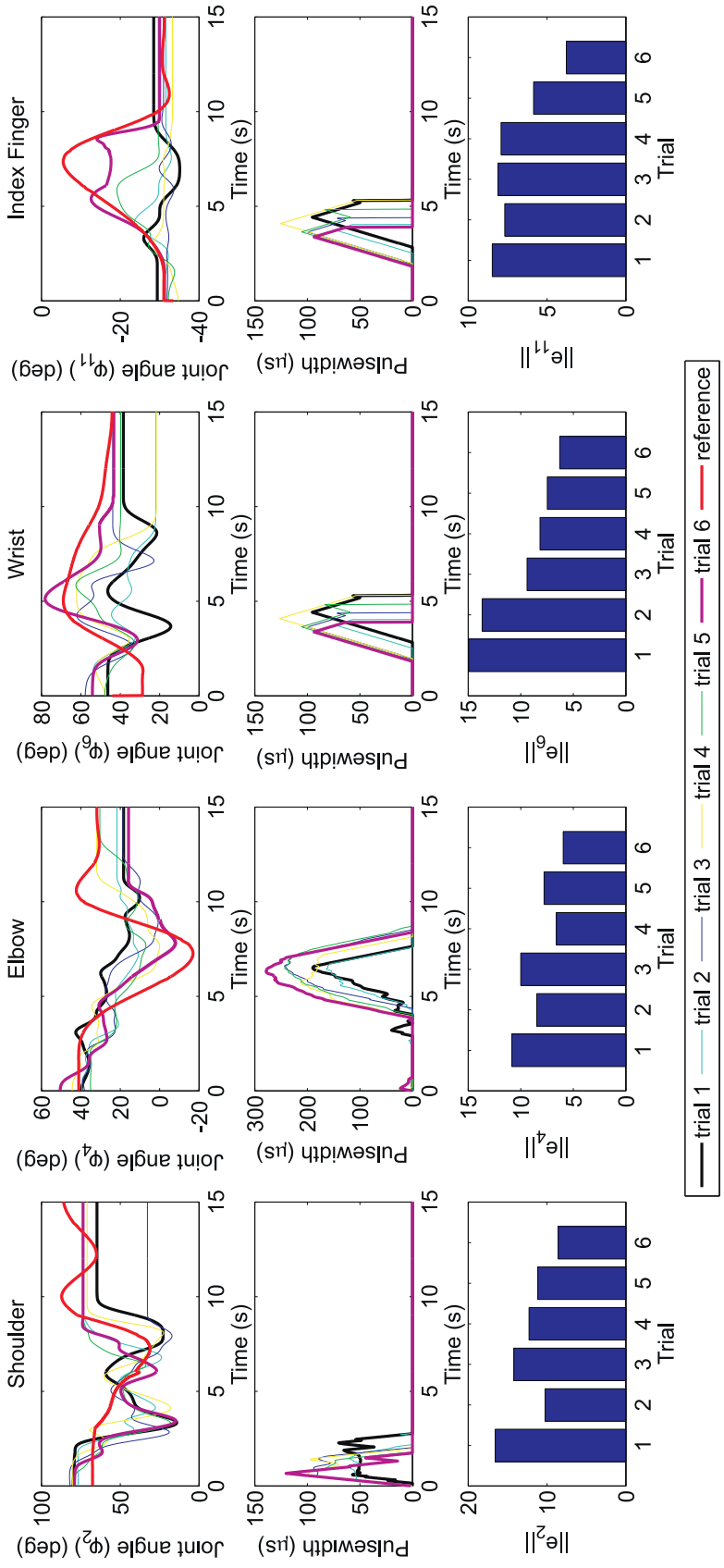

Fig. 9. Stroke Participant 1's tracking results for FES-Assisted drawer closing task.

Please cite this article as: M. Kutlu et al., Upper-limb stroke rehabilitation using electrode-array based functional electrical stimulation with sensing and control innovations, Medical Engineering and Physics (2016), http://dx.doi.org/10.1016/j.medengphy.2016.01.004

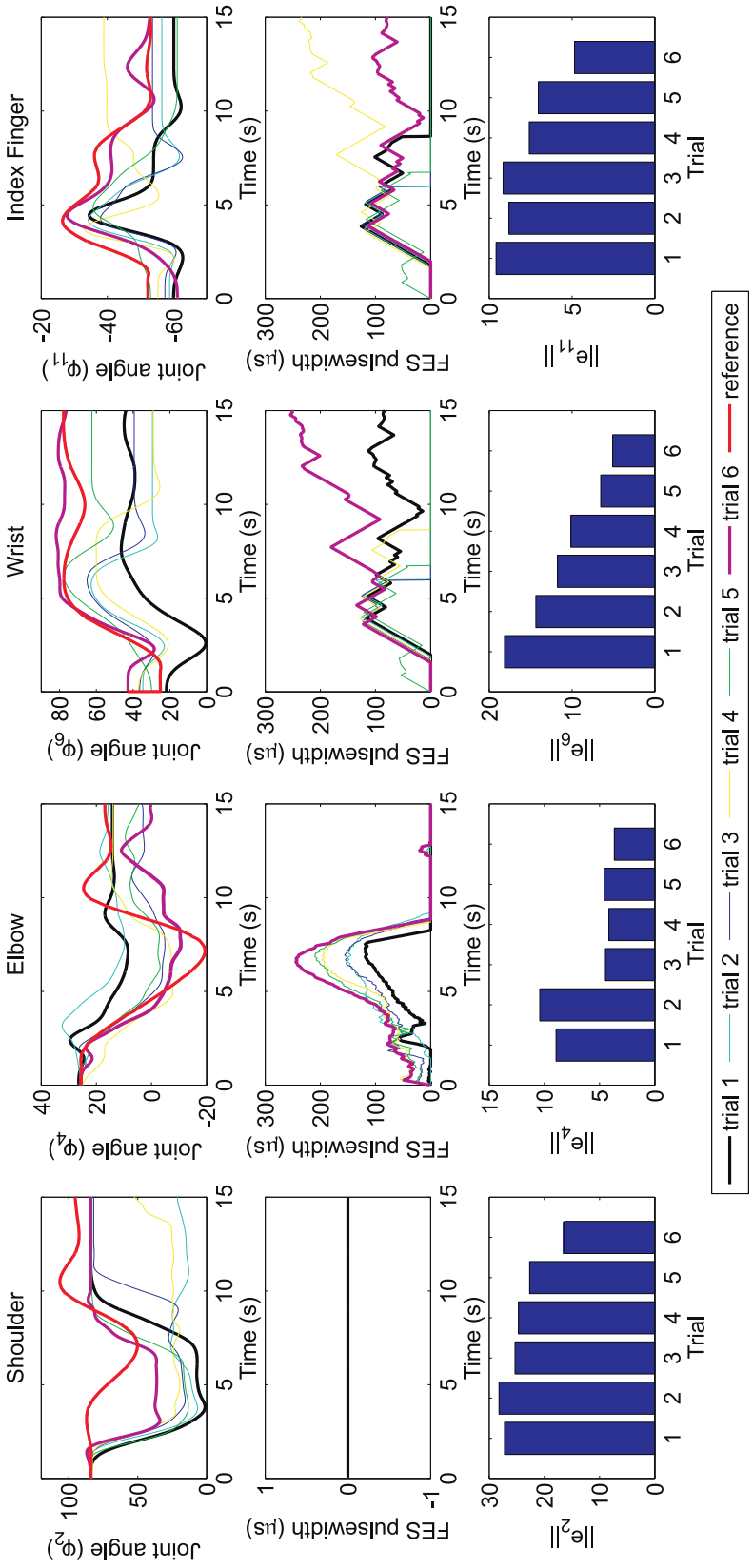

Fig. 10. Stroke Participant 4's tracking results for FES-Assisted low light task.

Please cite this article as: M. Kutlu et al., Upper-limb stroke rehabilitation using electrode-array based functional electrical stimulation with sensing and control innovations, Medical Engineering and Physics (2016), http://dx.doi.org/10.1016/j.medengphy.2016.01.004

Table 3
FES-assisted tracking results for stroke participants taken mid-way during intervention (session 9).

	Task	Trial no	Norm of error				
			$\|\hat{\phi}_2 - \phi_2\|$	$\|\hat{\phi}_4 - \phi_4\|$	$\|\hat{\phi}_6 - \phi_6\|$	$\|\hat{\phi}_{11} - \phi_{11}\|$	$\sum_{i=1}^{17} \|\hat{\phi}_i - \phi_i\|$
Participant 1	Drawer closing	1	16.6	10.8	14.9	8.47	192.8
		6	10.1	7.42	6.28	4.9	72.74
Participant 2	Far reaching	1	24.9	9.94	9.77	7.78	196.68
		6	19.1	5.01	5.36	6.52	89.12
Participant 3	Near reaching	1	16	5.42	30.4	12.5	186.84
		6	12	3.24	13.5	6.21	105.88
Participant 4	High light switch	1	25.3	8.68	12.9	9.55	217.96
		6	37.6	5.37	5.42	5.52	125.64

Table 4
Stroke participant clinical assessment data.

Participant	Action research Arm test		Fugl-Meyer		FES-unassisted range of movement							
					ϕ_2		ϕ_4		ϕ_6		ϕ_{11}	
	Baseline	Post	Baseline	Post	Baseline	Post	Baseline	Post	Baseline	Post	Baseline	Post
P1	8	9	26	33	6	14	30	33	30	50	11	23
P2	6	5	28	28	7	13	10	23	65	130	15	42
P3	7	3	30	35	2	16	16	29	59	73	6	44
P4	10	13	23	38	3	8	30	35	40	76	32	45
	t test p-value		0.1191		0.0264		0.0481		0.0596		0.0360	

5. Conclusion

Results confirm that FES, mediated by ILC, successfully assisted participants in completion of functional tasks, and training transferred to tangible changes in motor performance. The key findings were significant improvements in FES-unassisted performance with different metrics. In addition, participants reported that the system was usable, enjoyable and motivating, and importantly that the intervention was effective in reducing weakness, leading to changes in everyday activities at home. Finally, the feasibility of using low-cost, user-friendly sensing approaches and an arm support mechanism that can be used in conjunction with FES-assisted tasks was established. Future work will focus on translating the system into participants' homes, prior to conducting a randomised control trial.

Conflict of interest

None.

Acknowledgement

This work was supported by the Engineering and Physical Sciences Research Council (EPSRC) Grant no. EP/I01909X/1. Ethics Approval was given by University of Southampton Ethics and Research Governance Online (ERGO), ID 7710. We thank the people with stroke who participated in this study.

Appendix A. Selection of feedback controller $C_{c,w}$ and ILC operator L_w.

Design of feedback controller $C_{c,w}(s)$ for system $H_w(s) : \mu_k \mapsto \Phi_{w,k}$ is motivated by the form of muscle dynamics (7), which suggests that on the k^{th} trial a structure comprising a static 12×24 mapping combined with uniform dynamics may be used to represent the hand and wrist. In practice this assumption is supported by the presence of spasticity, inherent stiffness of the muscular tendon structure, and the low bandwidth of required movements. We therefore assume $H_w(s) = \bar{H}_w(s)P$ where P is a static mapping and $\bar{H}_w(s)$ is a SISO system, and introduce the control structure:

Proposition A.1. *The control action* $C_{c,w} : e_w \mapsto u_w : u_w = \bar{K}_w(s)(PW)^\dagger e_w$, *where* $\bar{K}_w(s)$ *is a SISO system, applied to system* $\Phi_w = \bar{H}_w(s)PWu_w$ *realises stimulation input*

$$u_w = N_w(s)u_w^\star \tag{A.1}$$

where $u_w^\star$ *minimises a weighted norm of the tracking error,* $e_w = \hat{\Phi}_w - \Phi_w$, *and the SISO system*

$$N_w(s) := (I + \bar{H}_w(s)\bar{K}_w(s))^{-1}\bar{H}_w(s)\bar{K}_w(s). \tag{A.2}$$

The resulting closed-loop dynamics are

$$\Phi_w = N_w(s)P_{PW}^{\perp}\hat{\Phi}_w. \tag{A.3}$$

where 12×12 *matrix* $P_{PW}^{\perp} = PW(PW)^\dagger$ *is the orthogonal projection onto the range of PW.*

Proof. Consider the weighted tracking error $u_w^\star = \min u_w \|\hat{\Phi}_w - \Phi_w\|_Q^2$ where weight $Q = (\bar{H}_w^{-1})^*\bar{H}_w^{-1}$ with $(\cdot)^*$ the adjoint operator. This has solution

$$\begin{aligned} u_w^\star &= \min u_w \|\hat{\Phi}_w - \Phi_w\|_Q^2 = \min_{u_w} \|\hat{\Phi}_w - \bar{H}_w PWu_w\|_Q^2 \\ &= \min_{u_w} \|\bar{H}_w^{-1}\hat{\Phi}_w - PWu_w\|^2 = (PW)^\dagger \bar{H}_w^{-1}\hat{\Phi}_w. \end{aligned} \tag{A.4}$$

where $(\cdot)^\dagger$ is the pseudo-inverse operator. The proposed control action $C_{c,w} = \bar{K}_w(s)(PW)^\dagger$ realises

$$\begin{aligned} u_w &= \bar{K}_w(PW)^\dagger(\hat{\Phi}_w - \bar{H}_w PWu_w) \Rightarrow (I + \bar{K}_w(PW)^\dagger \bar{H}_w PW)u_w \\ &= \bar{K}_w(PW)^\dagger\hat{\Phi}_w \Rightarrow (I + \bar{K}_w\bar{H}_w)u_w = \bar{K}_w(PW)^\dagger\hat{\Phi}_w \\ \Rightarrow u_w &= (I + \bar{K}_w\bar{H}_w)^{-1}\bar{K}_w(PW)^\dagger\bar{H}_w\bar{H}_w^{-1}\hat{\Phi}_w \Rightarrow u_w = N_w u_w^\star \end{aligned}$$

The corresponding closed-loop dynamics $G_w(s)$ are

$$\begin{aligned} \Phi_w &= \bar{H}_w PWu_w = \bar{H}_w PW(I + \bar{K}_w\bar{H}_w)^{-1}\bar{K}_w(PW)^\dagger\bar{H}_w\bar{H}_w^{-1}\hat{\Phi}_w \\ &= N_w(s)PW(PW)^\dagger\hat{\Phi}_w \end{aligned}$$

□

Control action $C_{c,w} = \bar{K}_w(s)(PW)^\dagger$ therefore provides a transparent method to achieve satisfactory tracking performance for all joints Φ_w. This requires only that SISO feedback controller $\bar{K}_w(s)$ be selected to stabilise dynamics (A.2) but ensures stability of all 12 joints. It also enables the following simplified ILC update design.

Proposition A.2. *When applied to the system of Proposition Appendix A.1, the ILC update structure*

$$v_{w,k+1} = v_{w,k} + L_w e_{w,k} \tag{A.5}$$

with operator $L_w = l_w(N_w P_{PW}^{\perp})^{\dagger}$, $l_w \in (0, 1]$, *enforces convergence to the minimum error norm, i.e.*

$$\lim_{k\to\infty} v_k = v^{\star}, \quad v^{\star} = \min_{v} \|\hat{\Phi}_w - \Phi_w\|^2. \tag{A.6}$$

Furthermore, if $\bar{K}_w(s)$ *is tuned so that* $N_w(s)$ *is a pure delay of* λ_w *seconds then* $L_w = l_w(N_w P_{PW}^{\perp})^{\dagger} = l_w e^{s\lambda_w}(P_{PW}^{\perp})^{\dagger} = l_w e^{s\lambda_w}(PW)^{\dagger}$, *and (A.5) is equivalent to the phaselead update*

$$v_{w,k+1}(t) = v_{w,k}(t) + l_w(PW)^{\dagger} e_w(t + \lambda_w) \tag{A.7}$$

Proof. Substitute $L_w = l_w(N_w P_{PW}^{\perp})^{\dagger}$ and $G_w = N_w(s)P_{PW}^{\perp}$ into limiting error solution $(I - G_w(L_w G_w)^{-1}L_w)\hat{\Phi}_w$ to give $(I - P_{PW}^{\perp})\hat{\Phi}_w$ which is the orthogonal projection onto the nullspace of $\hat{\Phi}_w$. This is the minimum achievable error and hence solves (A.6). If $N_w(s) = e^{-s\lambda_w}$ then $L_w = l_w(e^{-s\lambda_w}P_{PW}^{\perp})^{\dagger} = l_w e^{s\lambda_w}(P_{PW}^{\perp})^{\dagger} = l_w e^{s\lambda_w}(PW)^{\dagger}$ with time-based implementation (A.7). □

References

[1] Townsend M, Wickramasinghe N, Bhatnagar K, Smolina P, Nichols K, Leal M, et al. Coronary heart disease statistics Tech. Rep.. British Heart Foundation; 2012.
[2] Party ISW. National clinical guideline for stroke. Tech. Rep.. London: Royal College of Physicians; 2012.
[3] Desrosiers J, Malouin F, Richards C, Bourbonnais D, Rochette A, Bravo G. Comparison of changes in upper and lower extremity impairments and disabilities after stroke. Int J Rehabil Res 2003;26(2):109–16.
[4] Ingram JN, Körding KP, Howard IS, Wolpert DM. The statistics of natural hand movements. Exp Brain Res 2008;188(2):223–36.
[5] Kwakkel G, Kollen BJ, van der Grond J, Prevo AJ. Probability of regaining dexterity in the flaccid upper limb impact of severity of paresis and time since onset in acute stroke. Stroke 2003;34(9):2181–6.
[6] Kwakkel G. Impact of intensity of practice after stroke: issues for consideration. Disabil Rehabil 2006;28(13-14):823–30.
[7] Van Peppen RP, Kwakkel G, Wood-Dauphinee S, Hendriks HJ, Van der Wees PJ, Dekker J. The impact of physical therapy on functional outcomes after stroke: what's the evidence? Clin Rehabil 2004;18(8):833–62.
[8] de Kroon J, van der Lee J, IJzerman M, Lankhorst G. Therapeutic electrical stimulation to improve motor control and functional abilities of the upper extremity after stroke: a systematic review. Clin Rehabil 2002;16(4):350–60.
[9] Urton ML, Kohia M, Davis J, Neill MR. Systematic literature review of treatment interventions for upper extremity hemiparesis following stroke. Occup Ther Int 2007;14(1):11–27.
[10] de Kroon JR, Ijzerman MJ, Chae J, Lankhorst GJ, Zilvold G. Relation between stimulation characteristics and clinical outcome in studies using electrical stimulation to improve motor control of the upper extremity in stroke. J Rehabil Med 2005;37(2):65–74.
[11] Arya KN, Pandian S, Verma R, Garg R. Movement therapy induced neural reorganization and motor recovery in stroke: a review. J Bodyw Mov Ther 2011;15(4):528–37.
[12] Burridge JH, Ladouceur M. Clinical and therapeutic applications of neuromuscular stimulation: a review of current use and speculation into future developments. Neuromodulation 2001;4(4):147–54.
[13] Rushton DN. Functional electrical stimulation and rehabilitation an hypothesis. Med Eng Phys 2003;25(1):75–8.
[14] Zhang D, Guan TH, Widjaja F, Ang WT. Functional electrical stimulation in rehabilitation engineering: a survey. i-CREATe. New York, USA: ACM; 2007. p. 221–6.
[15] Lynch CL, Popovic MR. Functional electrical stimulation. IEEE Control Syst Mag 2008;28(2):40–50.
[16] Mangold S, Schuster C, Keller T, Zimmermann-Schlatter A, Ettlin T. Motor training of upper extremity with functional electrical stimulation in early stroke rehabilitation.. Neurorehabil Neural Repair 2009;23(2):184–90.
[17] Pelton T, van Vliet P, Hollands K. Interventions for improving coordination of reach to grasp following stroke: a systematic review. Int J Evid Based Healthc 2012;10(2):89–102.
[18] Hara Y, Ogawa S, Tsujiuchi K, Muraoka Y. A home-based rehabilitation program for the hemiplegic upper extremity by power-assisted functional electrical stimulation. Disabil Rehabil 2008;30(4):296–304.
[19] Kurosawa K, Futami R, Watanabe T, Hoshimiya N. Joint angle control by FES using a feedback error learning controller. IEEE Trans Neural Syst Rehabil Eng 2005;13(3):359–71.
[20] Nathan RH. Closed-loop control of the upper limb. In: Proceedings of 10th Annual Conference of the IFESS. Montreal, Canada; 2005. p. 1–3.
[21] Klauer C, Schauer T, Reichenfelser W, Karner J, Zwicker S, Gandolla M, et al. Feedback control of arm movements using neuro-muscular electrical stimulation (NMES) combined with a lockable, passive exoskeleton for gravity compensation. Front Neurosci 2014;8:1–16.
[22] Blana D, Kirsch RF, Chadwick EK. Combined feedforward and feedback control of a redundant, nonlinear, dynamic musculoskeletal system. Med Biol Eng Comput 2009;47(5):533–42.
[23] Hughes AM, Freeman CT, Burridge JH, Chappell PH, Lewin PL, Rogers E. Feasibility of iterative learning control mediated by functional electrical stimulation for reaching after stroke.. Neurorehabil Neural Repair 2009;23(6):559–68.
[24] Meadmore KL, Exell T, Hallewell E, Hughes A-M, Freeman CT, Kutlu M, et al. The application of precisely controlled functional electrical stimulation to the shoulder, elbow and wrist for upper limb stroke rehabilitation: a feasibility study. J NeuroEng Rehabil 2014;11(105):1–11.
[25] Meadmore KL, Hughes A-M, Freeman CT, Cai Z, Tong D, Burridge JH, et al. Functional electrical stimulation mediated by iterative learning control and 3D robotics reduces motor impairment in chronic stroke. J NeuroEng Rehabil 2012;9(32):1–11.
[26] Popovic-Maneski L, Kostic M, Bijelic G, Keller T, Mitrovic S, Konstantinovic L, et al. Multi-pad electrode for effective grasping: design. IEEE Trans Neural Syst Rehabil Eng 2013;21(4):648–54.
[27] Micera S, Keller T, Lawrence M, Morari M, Popovic DB. Wearable neural prostheses. IEEE Eng Med Biol Mag 2010;29(3):64–9.
[28] Heller BW, Clarke AJ, Good TR, Healey TJ, Nair S, Pratt EJ, et al. Automated setup of functional electrical stimulation for drop foot using a novel 64 channel prototype stimulator and electrode array: results from a gait-lab based study. Med Eng Phys 2013;35(1):74–81.
[29] Malešević NM, Maneski LZP, Ilić V, Jorgovanović N, Bijelić G, Keller T, et al. A multi-pad electrode based functional electrical stimulation system for restoration of grasp. J NeuroEng Rehabil 2012;9(66):1–12.
[30] Freeman CT. Electrode array-based electrical stimulation using ILC with restricted input subspace. Control Eng Pract 2014;23(2):32–43.
[31] Veerbeek JM, van Wegen E, van Peppen R, van der Wees PJ, Hendriks E, Rietberg M, et al. What is the evidence for physical therapy poststroke? A systematic review and meta-analysis.. PLoS ONE 2014;9(2):1–33.
[32] Levin MF. Interjoint coordination during pointing movements is disrupted in spastic hemiparesis. Brain 1996;119(1):281–93.
[33] Webster D, Celik O. Systematic review of kinect applications in elderly care and stroke rehabilitation. J NeuroEng Rehabil 2014;11(1):1–24.
[34] Lee G. Effects of training using video games on the muscle strength, muscle tone, and activities of daily living of chronic stroke patients. J Phys Ther Sci 2013;25(5):595–7.
[35] Clark RA, Pua Y-H, Fortin K, Ritchie C, Webster KE, Denehy L, et al. Validity of the Microsoft Kinect for assessment of postural control. Gait & Posture 2012;36(3):372–7.
[36] Dutta T. Evaluation of the Kinect sensor for 3-D kinematic measurement in the workplace.. Appl Ergon 2012;43(4):645–9.
[37] Metcalf CD, Robinson R, Malpass AJ, Bogle TP, Dell TA, Harris C, et al. Markerless motion capture and measurement of hand kinematics: validation and application to home-based upper limb rehabilitation. IEEE Trans Biomed Eng 2013;60(8):2184–92.
[38] Martin R, Lorbach M, Brock O. Deterioration of depth measurements due to interference of multiple RGB-D sensors. In: IEEE/RSJ International Conference on Intelligent Robots and Systems. Chicago, USA; 2014. p. 4205–12.
[39] Freeman CT, Tong D, Meadmore KL, Cai Z, Rogers E, Hughes AM, et al. Phase-lead iterative learning control algorithms for functional electrical stimulation-based stroke rehabilitation. Proc Inst Mech Eng Part I: J Syst Control Eng 2011;225(6):850–9.
[40] Le F, Markovsky I, Freeman CT, Rogers E. Identification of electrically stimulated muscle models of stroke patients. Control Eng Pract 2010;18(4):396–407.
[41] Bernotas LA, Crago PE, Chizeck HJ. A discrete-time model of electrcally stimulated muscle. IEEE Trans Biomed Eng 1986;33(9):829–38.
[42] Freeman CT. Upper limb electrical stimulation using input-output linearization and iterative learning control. IEEE Trans Control Syst Technol 2015;23(4):1546–54.
[43] Al-Gburi A, French M, Freeman CT. Robustness analysis of nonlinear systems with feedback linearizing control. In: 52nd IEEE Conference on Decision and Control. Florence, Italy; 2013. p. 3055–60.
[44] Freeman CT, French M. Multiple model approaches to iterative learning control. In: 54th IEEE Conference on Decision and Control. Osaka, Japan; 2015. p. 6070–5.
[45] Freeman CT, Exell T, Meadmore KL, Hallewell E, Hughes A-M. Computational models of upper limb motion during functional reaching tasks for application in FES based stroke rehabilitation. Biomed Eng J 2015;60(3):179–91.
[46] Freeman CT. Control system design for electrical stimulation in upper limb rehabilitation. Switzerland: Springer International Publishing; 2016.
[47] Mann G, Taylor P, Lane R. Accelerometer-triggered electrical stimulation for reach and grasp in chronic stroke patients a pilot study. Neurorehabil Neural Repair 2011;25(8):774–80.
[48] O'Dwyer SB, O'Keeffe D, Coote S, Lyons GM. An electrode configuration technique using an electrode matrix arrangement for FES-based upper arm rehabilitation systems. Med Eng Phys 2006;28(2):166–76.
[49] Brend O, Freeman CT, French M. Multiple model adaptive control of functional electrical stimulation. IEEE Trans Control Syst Technol 2015;23(5):1901–13.

Please cite this article as: M. Kutlu et al., Upper-limb stroke rehabilitation using electrode-array based functional electrical stimulation with sensing and control innovations, Medical Engineering and Physics (2016), http://dx.doi.org/10.1016/j.medengphy.2016.01.004